PROTEINS: Structure, Function, and Genetics 1:74–80 (1986)

The Galactan-Binding Immunoglobulin Fab J539: An X-Ray Diffraction Study at 2.6-Å Resolution

Se Won Suh,[1] T.N. Bhat,[1] Manuel A. Navia,[1] Gerson H. Cohen,[1] D.N. Rao,[2] Stuart Rudikoff,[2] and David R. Davies[1]
[1]*Laboratory of Molecular Biology, National Institute of Diabetes, Digestive and Kidney Diseases and* [2]*Laboratory of Genetics, National Cancer Institute, Bethesda, Maryland 20892*

ABSTRACT **The crystal structure of the Fab of the galactan-binding immunoglobulin J539 (a mouse IgA,κ) has been determined at a resolution of approximately 2.6 Å by X-ray diffraction. The starting model was that obtained from the real space search described previously (Navia, M.A., Segal, D.M., Padlan, E.A., Davies, D.R., Rao, D.N., Rudikoff, S. and Potter, M. "Crystal structure of galactan-binding mouse immunoglobulin J539 Fab at 4.5 Å resolution." Proc. Nat. Acad. Sci. USA, 76:4071–4074, 1979). This Fab structure has now been refined by restrained least-squares procedures to an R-value of 19% for the 11,690 unique reflections between 8.0 Å and 2.6 Å. The rms deviation from ideal bond lengths is 0.025 Å. The overall structure differs from McPC603 Fab, another mouse IgA,κ antibody, in that the elbow bend, relating the variable and constant parts of the molecule, is 145° vs. 133° for McPC603. The region of the molecule expected to be the antigen binding site contains a large cavity with two clefts leading away from it. This has been fitted with a model of an oligo-galactan.**

Key words: antibody, crystal structure, anti-galactan, J539

INTRODUCTION

Current knowledge of the three-dimensional structure of antibodies is based mostly on the X-ray diffraction investigations of fragments.[1,2] The structures of three Fabs have been determined: Kol [3] and New,[4] two human myeloma proteins, and McPC603,[5,6] a mouse IgA,κ protein. Of these, New and McPC603 have known binding specificities, while the specificity of Kol is not known. There is therefore only limited information available concerning the interaction of antibodies with their antigenic determinants. In this paper we describe the crystal structure determination of J539, a mouse immunoglobulin Fab with binding specificity for β(1–6)-D-galactan. J539 is a member of a group of several antigalactans whose binding properties have been extensively studied. It is the only carbohydrate-binding antibody to have been so far studied by X-ray diffraction.

Previously the structure of J539 Fab had been analyzed at low resolution.[7] There, a poorly defined 4.5-Å electron density map was examined by using a search procedure based on the known structure of McPC603 Fab. This analysis confirmed the overall similarity of these two Fab structures and provided a basis for the higher-resolution analysis reported here.

MATERIALS AND METHODS

Crystallization and Data Collection

J539 Fab was prepared as described previously,[8] except that the purified material was further subjected to preparative isoelectric focusing in order to produce material that would ultimately yield large crystals suitable for the production of high-resolution X-ray diffraction data.[9] The crystallizations were carried out by the hanging drop method at room temperature by using the vapor diffusion technique to equilibrate the protein droplet with a solution containing approximately 35% saturated ammonium sulfate, 0.07 M imidazole, 0.03 M zinc sulfate, pH 6.8. The crystals were orthorhombic, space group $P2_12_12_1$, with a = 54.1 Å, b = 74.2 Å, c = 130.8 Å.[7]

Intensity data were collected by rotation photography[10] on Kodak No-Screen Medical X-ray films by using an Elliott GX-6 rotating anode X-ray generator operating at 40 kV and 40 mA. A Franks double-bent mirror system[11] purchased from Brandeis University was used to focus the X-ray beam. Data were collected on an Enraf-Nonius Arndt-Wonacott rotation camera with a nominal 80-mm crystal-to-film distance. The c-axis of the crystal was parallel to the rotation axis of the camera and the rotation range for each film pack was 2.3° with 0.3° overlap between film packs. This range permitted us to discard the partially recorded reflections. A total rotation of 91° was sufficient to record all the independent reflections, except for those in the cusp along the c-axis. Precession camera data for the layers 0kl, 1kl, h0l, h1l, h2l, hk0, hk1, and hhl were also collected to assist in interfilm scaling and to supply some of the remaining unobserved reflections.

Received June 3, 1986; accepted June 16, 1986.

S.W. Suh is now at the Department of Chemistry, College of Natural Sciences, Seoul National University, Seoul, Korea.

M.A. Navia is now at the Merck Sharpe and Dohme Research Laboratories, Rahway, NJ 07065.

Address reprint requests to D.R. Davies, Laboratory of Molecular Biology, National Institute of Diabetes, Digestive and Kidney Diseases, Bethesda, MD 20892.

PUBLISHED 1986 BY ALAN R. LISS, INC.

The films were scanned at 100-μm raster steps on an Optronics P-1000 film scanner. The resulting digital data were processed on a VAX 11/780 computer with a rotation film program written by G. Cornick and M.A. Navia (unpublished work), which incorporated the dynamic mask procedure of Sjolin and Wlodawer[12] to extract the integrated intensities of reflections. The program was modified to allow the use of roughly measured coordinates of eight strong, fully recorded reflections as supplementary fiducial marks in obtaining the initial [Q] matrix.[13] This provided a starting transformation for a more accurate determination of the [Q] matrix by a least-squares procedure based on all fully recorded reflections which met certain criteria.

Intensities from the three films in each pack were first scaled, corrected for Lorentz and polarization factors, and symmetry averaged. Data from individual packs were merged and scaled together with those from the set of zero- and upper-level precession films by using a program of Y. Satow (unpublished work). The current data set to 2.6-Å resolution contains 81% of the possible reflections: 90% to 3.0-Å resolution and 64% between 3.0-Å and 2.6-Å resolution. Approximately 77% of the independent reflections were measured more than once. The statistics of the data processing are given in Table I.

Generation and Refinement of the Model

The location and orientation of the starting model[7] were confirmed using the rotation method[14] and an R-value search.[15,16] Initial refinement of the model was carried out by using CORELS. [17] Six parameters defining the orientation and position of the molecule were refined by using 10-Å to 7-Å data. Then constant and variable domains were refined as separate rigid groups by using 10-Å to 5.4-Å data. No noticeable improvement in the R-value was obtained when light and heavy chains were also treated as separate rigid groups.

This model was then refined with 3.5-Å data by using PROLSQ.[18,19] Residues of Fv were "mutated" from the McPC603 original model to those appropriate for J539 during the course of refinement. As the phases improved higher-resolution data were incorporated to the limit of 2.6 Å and the J539 sequence was substituted for the McPC603 residues. The sequence used was that of Rudikoff et al.[20] for VL, Rao et al.[21] for VH, Svasti and Milstein[22] and Hamlyn et al.[23] for CL and Auffray et al.[24] for CH1.

Initial model building was done by using the interactive graphics program BILDER[25] to fit the model to 2Fo-Fc and ΔF maps. With the availability of the OMITMAP procedure[26] the graphics program FRODO[27] was used to fit the model to an OMITMAP. This improved the location of a number of residues and the overall constrast in the maps increased along with the improvement in the phases. During the final passes of model building, 304 water molecules were added.

TABLE I. Statistics from Processing of the Film Data

Total number of reflections measured	37,222
No. of independent reflections	12,670
Interfilm scaling R-value*	0.077

*$R = \sum_h \sum_i |I_{hi} - \bar{I}_h| / \sum_h \sum_i I_{hi}$, where $\bar{I}_h$ is the average intensity for a given reflection and I_{hi} isone of the measurements which were averaged to yield $\bar{I}_h$.

The result of the final refinement cycle is summarized in Table II. The rms error in positional parameters was estimated to be 0.3 Å by the method of Luzzati.[28] The coordinates and other relevant data have been deposited in the Brookhaven Protein Data Bank.[29] Table III shows the relationship of the serial numbering system which we have used in this work to the system used by Kabat.[30]

RESULTS

In Figure 1 is drawn the carbon alpha skeleton of the J539 Fab. In overall appearance it resembles the structure of other Fabs, in particular McPC603. The pairs of domains, CH1 and CL, are quite similar, having 88 carbon alphas match to give an rms difference of 1.8 Å. The relation between CH1 and CL is that of a screw axis with a rotation of 174° and a translation of 1.9 Å. Similarly, with VH and VL, 99 pairs of carbon alphas match with an rms deviation of 1.6 Å to give a rotation of 169.4° and 0.04-Å translation.

As expected from their sequence identity, the constant domains of J539 resemble quite closely the two corresponding domains of McPC603. The rms deviation of the backbone atoms is 1.6 Å (2.1 Å for all atoms). The relative disposition of CL and CH1 in J539 and McPC603 is not, however, exactly the same. For McPC603 the screw relation between CL and CH1 corresponds to a 169° rotation with a 2.6-Å translation. In the region of residues 131–139 (J539 numbering) there appears to be a major difference in the folding of the two CH1 domains. This region includes a proline residue that has been interpreted to be a cis-proline in McPC603 but trans- in J539. We do not know whether these differences are the result of an inadequate analysis of weak electron density or represent real differences in structure. We are undertaking a higher resolution study of J539 in order to attempt to clarify this situation.

The angle between the constant and variable pairs of domains differs between J539 (145°) and McPC603 (133°). This angle, the "elbow bend" of the Fab,[31,32] has been found to be quite variable in different Fabs, going from about 133° in New and McPC603 to as much as 170° in the Fab Kol,[3] probably signify-

TABLE II. Refinement Data

	Actual rms deviation†	Target σ
Average ΔF	92.6	‡
R-factor*	0.19	
No. of structure factors	11,690	
rms deviations from ideal distance (Å)		
Bond distance	0.025	0.030
Angle distance	0.052	0.040
Planar 1–4 distance	0.029	0.030
rms deviation from planarity (Å)	0.016	0.025
rms deviation from ideal chirality (Å^3)	0.199	0.150
rms deviation from permitted contact distances (Å)		
Single torsion contacts	0.219	0.500
Multiple torsion contacts	0.289	0.500
Possible hydrogen bond	0.269	0.500
rms deviation from ideal torsion angles (°)		
For planar group (0 or 180)	2.5	3.0
For staggered group (±60 or 180)	26.0	15.0
For orthonormal group (±90)	22.3	15.0

*$R = \sum_h ||F_o| - |F_c|| / \sum_h |F_o|$.

†rms = root mean square.

‡The weight chosen for the structure factor refinement, the "target σ" of ΔF, was modeled by the function $w = (1/\sigma)^2$ with $\sigma = 47 - 230 \times (\sin(\theta)/\lambda - 1/6)$.

ing flexibility in the polypeptide chains between V and C.

The interdomain contacts are summarized in Tables IV and V. These tables show, for each residue, the number of atom pairs in contact with residues of the other chain. A contact is defined as a distance which is less than the sum of the atomic van der Waals radii[33] plus 1.0Å. Similar tables have been published for the McPC603 Fab[6] and we note that while the contacts between CL and CH1 are relatively preserved, the contacts between VL and VH contain significant differences, perhaps because of differences in the hypervariable regions. In J539 some 32 out of 86 interactions (37%) involve hypervariable residues only, compared with 46 out of 105 (44%) in McPC603. However, many of the same conserved residues found by Novotny and Haber[34] are also found here, making contacts across the interface. These include Y35, Q37, Y86, and F97 of the light chain and Q39, L45, W47, Y95, and W108 of the heavy chain.

TABLE III. Correspondence Between the Numbering Scheme Used Here and That of Kabat et al.[30]

Light chain		Heavy chain	
This paper	Kabat et al.	This paper	Kabat et al.
1–27	1–27	1–52	1–52
28–213	29–214	53	52a
		54–83	53–82
		84–86	82a–82c
		87–104	83–100
		105	100a
		106–135	101–130
		136–138	133–135
		139–159	137–157
		160–167	162–169
		168–180	171–183
		181–196	185–200
		197–201	202–206
		202–212	208–218
		213–218	220–225

The Galactan Binding Site

The binding of galactan in J539 has been extensively studied in solution by Glaudemans and his coworkers. The antibody combining site was shown to accommodate four sequential β(1–6)-galactopyranosyl residues.[35–37] Recently, Glaudemans et al.[38] have concluded from a binding study of a number of deoxyfluorogalactosides that the binding involves both of the two solvent-exposed tryptophans in the combining site (residues W92L and W33H). They also proposed a rather specific model for the orientation of the galactan on the surface of the antibody molecule.

In this crystal form of J539 the presumed binding site for galactan is in close proximity to the constant region of a neighboring molecule (Table VI). Probably because of this close contact our attempts to diffuse galactan into these crystals were unsuccessful. Thus we have no direct crystallographic evidence to define the binding pocket of the Fab. Nevertheless, the three-dimensional structure of the variable module does provide some clues. Figure 2 is a skeletal model of J539 showing just the complementarity determining

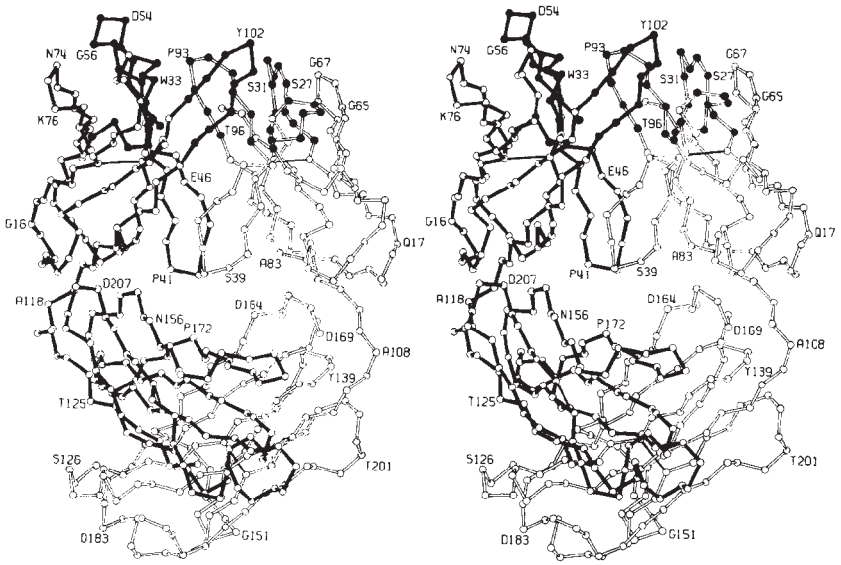

Fig. 1. A stereo drawing of the alpha carbon skeleton of J539 Fab. Solid bonds indicate the heavy chain. Filled circles show the complementarity determining residues.[30]

residues. A large pocket formed mainly by the CDRs of the light and heavy chain can be seen clearly, and connected to it there are two grooves. The bottom of the pocket is formed mainly by residues I95L, E50H, and L99H. Residues W33H, H52H, W90L, and Y92L line the side of the pocket. Residues Y101H, Y104H, and Y92L form the outer surface of the pocket. Residues Y92L and P93L partition the large pocket into one central deep pocket and two clefts on either side. Residues S30L, T91L, and Y92L form one of these clefts and W33H, D54H, Y92L, and H52H form the other cleft.

Binding experiments[39] demonstrate that J539 binds to the middle of the galactan polymer, rather than at the ends. Accordingly, we have examined models constructed by placing several galactan residues partly in the central cavity with the chain extending away from the cavity in both directions along the two grooves.

Several conformations of galactan could be reasonably fitted to the binding pocket based on a consideration of van der Waals contacts alone. They could be constructed with the carbohydrate chain running in either direction. One of these, shown in Figure 3, is

TABLE IV. Contacts Between Residues of VL and VH*

		V37	Q39	G44	L45	W47	E50	H52	N59	Y60	P62	Y95	L99	Y104	N105	W108	G109
E	1	·	·	·	·	·	·	·	·	·	1	·	·	·	·	·	·
H	33	·	·	·	·	·	·	·	·	·	·	·	·	2	1	·	·
Y	35	·	·	·	·	·	·	·	·	·	·	·	·	·	3	2	·
Q	37	·	4	·	·	·	·	·	·	·	·	·	·	·	·	·	·
S	42	·	·	·	·	·	·	·	·	·	·	1	·	·	·	·	1
P	43	·	·	·	1	·	·	·	·	·	·	2	·	·	·	11	·
P	45	·	·	·	·	·	·	·	·	·	·	·	·	·	·	4	·
Y	48	·	·	·	·	·	·	·	·	·	·	·	·	4	8	·	·
Y	86	·	·	1	·	·	·	·	·	·	·	·	·	·	·	·	·
W	90	·	·	·	·	·	·	·	·	·	·	·	1	7	8	·	·
Y	92	·	·	·	·	·	·	2	3	·	·	·	·	·	·	·	·
P	93	·	·	·	·	·	1	·	·	·	·	·	·	·	·	·	·
L	94	·	·	·	·	1	·	·	3	3	1	·	·	·	·	·	·
I	95	·	·	·	·	5	·	·	·	·	·	·	·	·	·	·	·
F	97	2	·	·	2	·	·	·	·	·	·	·	·	·	·	1	·

*Residues listed in the left column are from VL; the residues listed above the columns are from VH. The numbers in the table correspond to the number of pairs of atoms from two residues which are within potential van der Waals contact distance. A dot (·) indicates no contacts. The boxed regions delineate possible hypervariable to hypervariable interactions.

TABLE V. Contacts Between Residues of CL and CH1*

		Y127	P128	L129	T130	L131	P132	P133	I141	L145	H147	F171	P172	A174	Q186
S	115	·	·	·	·	·	·	·	2	·	·	·	·	·	·
I	116	·	·	·	·	·	4	·	·	·	·	·	·	·	·
F	117	·	·	6	2	·	16	2	2	·	·	·	·	·	·
S	120	·	1	·	·	·	·	·	·	·	·	·	·	·	·
E	122	2	3	·	·	·	·	·	·	·	·	·	·	·	·
Q	123	12	·	·	·	·	·	·	·	·	2	·	·	·	·
S	126	1	·	·	·	·	·	·	·	·	·	·	·	·	·
S	130	·	·	·	·	·	·	·	·	1	·	·	·	·	·
V	132	·	·	1	·	·	·	·	·	·	·	·	·	·	·
F	134	·	·	·	·	·	·	·	·	·	·	4	·	·	5
N	136	·	·	·	·	·	·	·	·	·	·	·	·	·	4
L	159	·	·	·	·	·	·	·	·	·	·	·	·	2	·
N	160	·	·	·	·	·	·	·	·	·	·	·	·	1	·
S	161	·	·	·	·	·	·	·	·	·	·	·	2	1	·
W	162	·	·	·	·	·	·	·	·	·	·	·	2	·	·
T	163	·	·	·	·	·	·	·	·	·	·	2	·	·	·
S	173	·	·	·	·	·	·	·	·	·	·	3	·	·	·
M	174	·	·	·	·	·	·	·	·	·	·	1	·	·	·
S	175	·	·	·	·	·	·	·	·	·	·	3	·	·	·
E	212	·	·	·	·	5	·	·	·	·	·	·	·	·	·

*Residues listed in the left column are from CL; the residues listed above the columns are from CH1. The numbers in the table correspond to the number of pairs of atoms from two residues which are within potential van der Waals contact distance. A dot indicates no contacts.

similar in general terms to the model proposed by Glaudemans et al.[40] The preliminary and tentative nature of this model should be emphasized. It was constructed simply by fitting the galactan into the combining site in a manner that would avoid bad nonbonded contacts, but without taking into account possible hydrogen bonds and without minimizing the energy of contact. The great flexibility of the $\beta(1\text{–}6)$ carbohydrate linkage facilitates the fitting of these models but at the same time reduces the probability of obtaining a unique model. We are at present trying to grow crystals of J539 from solutions containing various oligogalactans; in this way we hope to observe directly, although probably in a different crystal form, the manner in which the antibody binds to the galactan.

TABLE VI. Contacts Between Residues of Two Molecules Related by a Twofold Screw Axis Parallel to the z Unit Cell Edge*

		Y92	H52	D54	S55	T57	H100	Y101	Y104
S	137	·	·	7	·	·	·	·	·
D	138	·	·	19	1	·	·	·	·
V	192	10	2	·	·	1	·	·	·
E	196	·	·	·	·	·	1	9	1

*Residues listed in the left column are from CH1 of one molecule; the residues listed above the columns are from a neighboring molecule and are from VL (Y92) and VH. The residues Y92L, H52H, D54H, Y101H, and Y104H are involved in the putative hapten binding pocket. The numbers in the table correspond to the number of pairs of atoms from two residues which are within potential van der Waals contact distance. A dot indicates no contacts.

Comparison With Predicted Models of J539

The variable region of J539 has been the subject of numerous modeling attempts. These have ranged from simple backbone models to fairly complete models for all the atoms in the combining site region[41,42] (Padlan, Glaudemans, and Davies, unpublished). We have compared several of these models with the observed structure derived from X-ray diffraction. Although in many of the CDR loops the models show quite good agreement with the X-ray structure, there are always some loops that show very poor agreement. As an example, we quote the comparison for the model proposed by Mainhart et al.,[41] whose coordinates were kindly given to us by Mainhart. We observe an rms deviation for the alpha carbons of 2.7 Å for all the heavy-chain CDRs and 1.8 Å for the light-chain CDRs. For the individual CDRs, the alpha carbon rms deviations range from 1.1 Å for H1 and L2 to 4.0 Å for H3. If all the atoms are included, then the deviations are 4.6 Å and 3.0 Å for the heavy- and light-chain CDRs, respectively. The rms deviations for the individual CDRs range from 2.0 Å and 2.1 Å for L1 and L2 to 3.9 Å for H1 and L3 and 6.5 Å for H3. Similar deviations are found in other predicted models. These large discrepancies between prediction and observation for key parts of the combining site, in spite of encouraging agreement in other parts, are probably due to inadequacies in the

DOCKET ALARM

Explore Litigation Insights

Docket Alarm provides insights to develop a more informed litigation strategy and the peace of mind of knowing you're on top of things.

Real-Time Litigation Alerts

Keep your litigation team up-to-date with **real-time alerts** and advanced team management tools built for the enterprise, all while greatly reducing PACER spend.

Our comprehensive service means we can handle Federal, State, and Administrative courts across the country.

Advanced Docket Research

With over 230 million records, Docket Alarm's cloud-native docket research platform finds what other services can't. Coverage includes Federal, State, plus PTAB, TTAB, ITC and NLRB decisions, all in one place.

Identify arguments that have been successful in the past with full text, pinpoint searching. Link to case law cited within any court document via Fastcase.

Analytics At Your Fingertips

Learn what happened the last time a particular judge, opposing counsel or company faced cases similar to yours.

Advanced out-of-the-box PTAB and TTAB analytics are always at your fingertips.

API

Docket Alarm offers a powerful API (application programming interface) to developers that want to integrate case filings into their apps.

LAW FIRMS
Build custom dashboards for your attorneys and clients with live data direct from the court.

Automate many repetitive legal tasks like conflict checks, document management, and marketing.

FINANCIAL INSTITUTIONS
Litigation and bankruptcy checks for companies and debtors.

E-DISCOVERY AND LEGAL VENDORS
Sync your system to PACER to automate legal marketing.